

Real-Time Multiple Particle Tracking of Gene Nanocarriers in Complex Biological Environments

Samuel K. Lai and Justin Hanes

Summary

Complex biological fluids, such as the vast and molecularly crowded cell cytoplasm and the highly viscoelastic mucus that protects many entry ways to the body, pose significant barriers to efficient gene delivery. Understanding the dynamics of gene carriers in such environments allows insight that leads to rational improvements in gene vector design. Fluorescence techniques that provide only ensemble-averaged transport characteristics do not provide detailed information related to the nature of various barriers to efficient gene vector transport to target cell nuclei. Multiple particle tracking (MPT) allows the tracking of the real-time motion of up to hundreds of individual particles simultaneously with high temporal and spatial resolution. We have adapted MPT to study gene carrier transport in live cells and in fresh, undiluted human mucus. By analyzing the displacements of gene vectors as a function of time scale, this technique provides, on a per particle basis, highly quantitative measurements of the transport rates and transport mechanisms, as well as biophysical information of the complex biological environments. Combining MPT with confocal microscopy (confocal particle tracking) allows dynamic and quantitative co-localization determination of gene carriers with various cellular structures, such as endosomes, lysosomes, the endoplasmic reticulum, and Golgi. We have applied MPT to enhance understanding of critical extracellular and intracellular bottlenecks to gene transfer.

Key Words: mucus; intracellular transport; polyethylenimine; polymers; polyplexes; fluorescence; drug delivery systems; active transport; diffusion.

1. Introduction

1.1. Extracellular and Intracellular Barriers to Gene Transfer

Biological environments present a multitude of barriers that can hinder the transfer of genes to the nucleus of targeted cells (1). The gene that could correct the CFTR defect responsible for Cystic Fibrosis (CF) was discovered in 1989, yet no patient has been cured (2). The Achilles heel to gene therapy for CF, as with most other diseases for which gene therapy holds promise, is the effective delivery of corrective genes through hordes of biological obstacles (3,4). For example, for gene therapy to be effective for CF in the lungs, gene vectors must first traverse lung mucus linings that typically serve to protect the underlying epithelia from the entry of foreign particles, such as pathogens and toxins (5,6). Mucus in the lungs, gastrointestinal tract, and cervicovaginal tract poses both steric obstruction, because of dense mesh structures, and adhesive interactions between mucin fibers (with both anionic and hydrophobic domains) and polymers and lipids often used for condensation of cargo plasmids (7). Upon cell entry, gene vector transport to the cell nucleus may also be hindered by the highly crowded cytoplasm, including dense cytoskeletal networks of actin and microtubules (8). The cell cytoplasm is particularly crowded near the cell nucleus, which may significantly hamper gene delivery even with particles that rapidly accumulate near the cell nucleus (8)–(10). For example, the transport of naked DNA larger than 2000 bp in the cytoplasm is strongly retarded, rendering even modest-sized DNA molecules essentially immobile (11).

In this chapter, multiple particle tracking (MPT) of gene carriers in extracellular and intracellular environments is described. The procedures cover the formation of fluorescent polymeric gene nanocarriers based on polyethylenimine (PEI), preparation of microscopy samples, collection of videos with high spatiotemporal resolution, and analysis of the motion of gene nanocarriers that yield information about their transport rates and mechanisms.

1.2. MPT: Theory and Applications

MPT involves resolving the dynamic motions of tens to hundreds of individual particles simultaneously in a given environment, such as a cell, using fluorescence video microscopy. The dynamic behavior of each gene vector yields quantitative information (e.g., effective diffusivities, maximum velocities, directionality) and qualitative information (e.g., mechanism of transport) that characterizes the transport of individual gene carriers. Tracking of individual particles also allows critical quantification of particle–environment interactions and biological processes that may dictate bulk transport properties.

In practice, because of current limitations in microscopy, it remains difficult to obtain 3D positional data with high temporal resolution. Therefore, the motions of gene carriers are typically tracked in 2D. 2D tracking provides accurate information on particle behavior if the biological environment (e.g., cell cytoplasm) is locally isotropic, but not necessarily homogeneous (**I**). Briefly, displacements of particles along the x , y , and z axes (Δx , Δy , Δz) are uncorrelated in a locally isotropic medium; hence, timescale-dependent ensemble 2D mean squared displacements [$\langle \Delta r^2(\tau) \rangle$ or MSD],

$$\langle \Delta r^2(\tau) \rangle_{2D} = \langle \Delta x^2 \rangle + \langle \Delta y^2 \rangle \quad (1)$$

is exactly equal to two-thirds of the timescale-dependent ensemble 3D MSD,

$$\langle \Delta r^2(\tau) \rangle_{3D} = \langle \Delta x^2 \rangle + \langle \Delta y^2 \rangle + \langle \Delta z^2 \rangle \quad (2)$$

because the ensemble displacements $\langle \Delta x^2 \rangle = \langle \Delta y^2 \rangle = \langle \Delta z^2 \rangle$.

Single particle tracking (SPT) was previously used to quantify the lateral movements of proteins and receptors on the cell surface (**12,13**), and the intracellular dynamics of adeno-associated viruses (AAV) (**14**). Over the past decade, advances in computational processing and image analysis software have afforded the development of MPT as a high throughput analog of SPT for rapid analysis of the movements of hundreds of particles simultaneously. MPT has been applied to the characterization of viscoelastic properties of various complex biological fluids (**15**) and the dynamic transport of gene complexes and model gene carriers in live cells and in fresh human mucus (**5,6,8**).

1.3. Modes of Transport in Biological Environments

The Brownian motion of particles in a purely viscous (i.e., not elastic) environment tracked in 2D can be described by the equation

$$\langle \Delta r^2(\tau) \rangle_{2D} = 4D_o\tau \quad (3)$$

where the time scale-independent diffusivity D_o is governed by the Stokes–Einstein relation $D_o = k_B T / 6\pi\eta a$, where k_B is the Boltzmann’s constant, T is the temperature, η is the fluid viscosity, and a is the particle radius. The key feature of unobstructed diffusion is that D_o is independent of time scale, τ . Thus, D_o can be obtained from $D_o = \langle \Delta r^2(\tau) \rangle_{2D} / 4\tau$ and purely diffusive Brownian motion can be identified by a slope of 1 on a MSD vs. τ plot.

In the presence of dense fiber networks, where the effective pore size approaches the size of gene carriers, particle motion can be impeded by steric obstruction. Adhesive interactions between gene vectors and fibers or other obstacles can further reduce diffusion. The hindered transport arising from these steric and adhesive forces can be characterized by

$$\langle \Delta r^2(\tau) \rangle_{2D} = 4D_o^\alpha \tau \quad (4)$$

where the value of α quantifies the extent of impediment ($0 < \alpha < 1$; smaller α values represent more strongly hindered transport) (16,17). In the case of strong interactions between gene vectors and fibers, the impediment may lead to displacements below the microscope's detection limit. We often refer to these vectors as immobile.

Gene vectors may also utilize motor proteins to achieve energy-dependent active transport. Active transport is characterized by large, directed

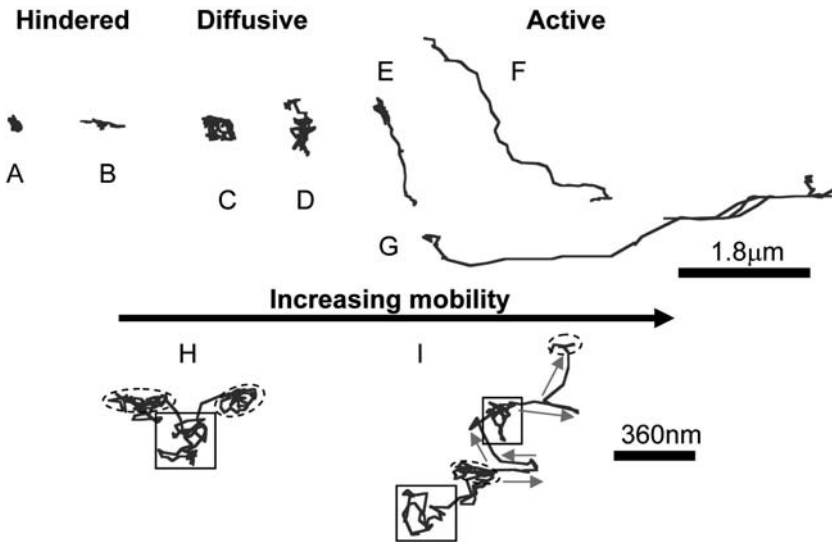


Fig. 1. Sample trajectories of nonviral polyethylenimine gene vectors undergoing different mechanisms of transport in live human cervical epithelial carcinoma HeLa cells. Gene vectors may undergo various mechanisms of transport: (A and B) diffusion that is substantially hindered by cellular components, (C and D) relatively unhindered diffusion, or (E–G) active transport characterized by directed displacements over great distances. (H and I) Gene vectors may display episodes of all three transport phenomena; hindered motions are outlined by dashed lines, diffusive motions by solid lines, and directed active motions by grey arrows. Scale bar is 1.8 μm for trajectories (A–I) and 360 nm for trajectories (H–J).

displacements and saltatory motions. The mean velocity, v , of facilitated transport is determined from the measured MSD of a particle through the relation

$$\langle \Delta r^2(\tau) \rangle_{2D} = 4D_0\tau + v^2\tau^2 \quad (5)$$

In the absence of facilitated transport mechanisms, (5) can be used to describe displacements influenced by convective bulk fluid flow.

In biological environments, it is rare that displacements of a group of particles over an extended period of time can be described by just one of the aforementioned mechanisms of transport. Even individual particles may experience episodes of hindered transport, free diffusion, and facilitated active transport (Figure 1). Using MPT and the concept of relative change in diffusivity (RC) (9,18), it is possible to quantitatively assign appropriate transport modes to hundreds of individual particles.

For more information on particle tracking for drug and gene delivery applications, the reader is referred to our recent review (1).

2. Materials

2.1. Cell Culture

1. Dulbecco's Modified Eagle's Medium (DMEM) supplemented with 10% fetal bovine serum (FBS). Store at 4°C.
2. Solution of trypsin (0.25%) and 1 mM ethylenediamine tetraacetic acid (EDTA). Store at 4°C.
3. Phosphate-buffered saline (PBS): dissolve 0.23 g anhydrous NaH_2PO_4 , 1.15 g anhydrous Na_2HPO_4 , and 8.75 g NaCl in 900 ml ddH₂O, correct pH to 7.4 using 1 M NaOH or 1 M HCl, and adjust volume to 1 l with ddH₂O. Autoclave; store at room temperature.
4. 0.4% w/v Trypan Blue solution (Gibco/BRL, Bethesda, MD, USA). Store at room temperature in dark.

2.2. Extracellular Fluids

The collection of various bodily fluids, including CF lung sputum, nasal or cervical vaginal mucus, should be performed by experts and should conform to protocols approved by the Institutional Review Boards at respective universities. To maximize biological relevance, dilution of samples at any point during the collection process should be minimized or avoided because dilution of mucus may lead to drastic changes in the micro- and macro-rheological properties. Fresh samples should be used for microscopy within 2 h of collection. Alternatively, mucus may be frozen for long-term storage at -20°C before use; however, the transport properties of control particles (100 nm PEG-modified

polystyrene) should be determined on fresh samples and on each thawed sample to ensure that the mucus structure has not been altered by freezing.

2.3. Fluorescently-Labeled Gene Complexes

1. 25 kDa branched PEI (Polysciences, Warrington, PA, USA). Prepare a 100 mg/ml solution in ddH₂O, pH 7.0. Store at room temperature.
2. DNA from salmon testes (~2 kDa; Sigma, St. Louis, MO, USA) or, alternatively, any plasmid DNA that does not express fluorescent proteins. Dissolve in ddH₂O to 1 mg/ml. Store at 4°C.
3. 1.0 M NaCl, pH 7.0. Store at room temperature.
4. 0.1 M sodium tetraborate, pH 9.3. Store at room temperature.
5. Oregon Green 514 carboxylic acid, succinimidyl ester (Molecular Probes, Eugene, OR, USA). Store at -20°C in dark, desiccated.
6. Dimethylsiloxane (DMSO). Store at room temperature.
7. 0.1 M sodium bicarbonate buffer. Store at room temperature.
8. G-75 Sephadex (Pharmacia, Piscataway, NJ, USA). Store at room temperature.
9. Trinitrobenzenesulfonic acid (TNBS; Sigma). Store at 4°C in dark.
10. Microcon Centrifugal Filter (100,000 Da cutoff; Millipore, Bedford, MA, USA).

2.4. Confocal Microscopy

1. Opti-MEM® Reduced Serum Media (Phenol red-free; Invitrogen, Carlsbad, CA, USA) Store at 4°C.
2. Hoechst 34580 Nucleic Acid label (Invitrogen). Store at 4°C in dark.
3. Glass bottom 35-mm culture dishes (Mattek Corp, Ashland, MA, USA)
4. Zeiss LSM 510 Meta Confocal Microscope with 100 × objective (Numerical Aperture 1.4) and excitation and emission filters for FITC (488 nm *ex*, 530 nm *em*) and UV (392 nm *ex*, 440 nm *em*). Other inverted fluorescence microscopes, such as the Zeiss Axiovert 100A, may be substituted for some studies. For live cell microscopy, a motorized stage (for collection of z-stack images) and a live cell chamber, such as Biotech FCS-2 Environmental Stages, are recommended. In this case, care must be taken to ensure that evaporation does not affect sample properties. Alternatively, a stage warmer, such as Nevtex, can be used to maintain temperature at 37°C. Microscopes are assumed to be fully functional, well aligned, and dimensions of pixels of the camera carefully measured. The ability to capture movies with high temporal and spatial resolution is solely dependent on the individual microscope setup and capability; readers are recommended to contact the microscope manufacturers for optimizing the microscope for MPT.

2.5. MPT

1. Glycerol. Store at room temperature.
2. Fluorescent latex beads (200 nm, COOH-modified, yellow-green fluorescent; Invitrogen). Store at 4°C in dark.

3. Labtek four-well Borosilicate chambered coverglass (Nalge Nunc International, Naperville, IL, USA).

2.6. Particle Tracking and Data Analysis Software

1. MetaMorph software 6.1 (Universal Imaging Co., Downingtown, PA, USA) with the Track Objects Application included. Other freely available software, such as ImageJ with the Particle Tracking plug-in, may be used instead.
2. Any programming software capable of manipulation of large data sets. Either Mathworks Matlab 7.0 or Microsoft Visual Studio C++ 6.0 is recommended.

3. Methods

3.1. Fluorescent Labeling of polyethylenimine

The experimental procedure given below describes the general steps needed for labeling common cationic polymers. It is possible to label the plasmid as well using various nucleic acid labels. Covalently attached fluorescent dyes are recommended for nucleic acids as intercalating dyes may label endogenous DNA instead. A few covalent DNA labels are listed in **Table 1**.

1. Preparing reagents:
 - a. Reagent A: Dissolve 1 mg OG-488 in 100 μ l DMSO. Use within 1 h.
 - b. Reagent B: Dilute 10 μ l stock 100mg/ml PEI in 490 μ l 0.1 M Na_2CO_3 .
2. Add Reagent A to Reagent B, vortex at lowest setting at room temperature in dark for 3 h. The end product is orange in color.
3. Prepare size exclusion chromatography column. Place 400 mg Sephadex in 125 ml ddH_2O , hydrate for 3 h at 90°C with occasional swirl. Cool for 15 min, then carefully transfer to column. Prep column with 3 volumes of water.
4. Add sample to column along with 10 ml ddH_2O . Sample passes through the gel through gravity flow. Collect eluent in 8–10 volume fractions (~1 ml each).
5. Identify collected volume fractions containing PEI through TNBS assay. First, establish a PEI standard curve by preparing a series of diluted PEI solutions from stock 100 mg/ml PEI solutions using 0.1 M sodium tetraborate to the range of 2.5–25 μ g/ml. 25 μ l of 0.3 M TNBS solution should be added to 1 ml of PEI solution, and absorbance on a spectrophotometer should be read at 511 nm, resulting in a linear fit within this range. Subsequently, the same TNBS assay is performed on eluent fractions diluted 1:300 in 0.1 M sodium tetraborate. PEI concentrations can be calculated by comparison to the standard curve. To confirm the calculations, the total amount of PEI from all eluent fractions should roughly equal 1 mg.

Table 1
Select Samples of Covalent Nucleic Acid Fluorescent Labels

Product	Fluorescence (ex, em)	Remarks
Alexa Fluor™ succinimidyl ester	AF 546: 556 nm, 573 nm AF 647: 650 nm, 668 nm	Requires DNA to be amine modified by reverse transcription in the presence of aminoallyl dUTP before conjugation with amine reactive dyes. Exceptional resistance to photobleaching
Ethidium monoazide bromide	510 nm, 605 nm	Photocrosslinking agent covalently binds to nucleic acid upon UV excitation
Label IT Tracker™	Cy™ 3: 553 nm, 575 nm Cy™ 5: 651 nm, 674 nm	Non-enzymatic chemical labeling of predominantly the N7 position of guanine
pGeneGrip™	Rhodamine: 540 nm, 590 nm Fluorescein: 490 nm, 525 nm	Covalent linkage of fluorophores through peptide nucleic acid clamps; expression of plasmid is not affected
ULYSIS Labeling Kit	OG488: 495 nm, 520 nm Pacific Blue: 410 nm, 455 nm	Similar labeling mechanism as Label IT Tracker™ and photobleaching resistance as Alexa Fluor™ succinimidyl ester

6. The degree of conjugation (DOC) can be quantified using the following equation:

$$DOC = (A_{511}) (DilutionFactor) / (70000) [PEI] \quad (6)$$

where [PEI] is expressed in moles per liter. Samples should be diluted 50× for absorbance measurements. Typically, DOC is in the range of 10–20 dye molecules per molecule PEI.

3.2. Tracking Latex Beads in Glycerol (To Determine Tracking Resolution)

1. Prepare a small aliquot of 1:100 diluted 200 nm latex beads from stock solution in ddH₂O (final w/v 0.02%).
2. Add 25 μ l of diluted particle solution to 1 ml glycerol in an eppendorf tube. The exact volume of glycerol is not critical. Wrap the sample in aluminum foil and vortex overnight.
3. Carefully transfer 600 μ l of glycerol with particles to one of the chambers in a 4-well glass chamber slide, taking care to minimize formation of air bubbles. Equilibrate at room temperature in dark for 2 h.
4. Visualize the sample under fluorescence microscope (add oil if using an objective that requires lens oil). The plane of focus should be at least 10 μ m above the bottom glass surface to ensure microscopy of particles in glycerol. Carefully look for convective motions along any one direction, if any. Using a 512 \times 512 silicon-intensified target camera (0.23 μ m/pixel), approximately 10–20 particles should be in view of focus. Adjust fluorescence intensity and detector gain to maximize signal-to-noise and minimize intensity saturation.
5. Carefully record 20–40-s movies at maximum temporal resolution. Very few, if any, particles become out of focus over the duration of microscopy (*see Note 1*). Pixel binning should be avoided to maximize the tracking resolution. A minimum of 20–30 movies should be collected for analysis. Movies should be saved as 16-bit TIFF format to prevent loss of information.

3.3. Preparation of Cells for Microscopy

1. Human cervical epithelia carcinoma cells (HeLa) should be passed and plated onto 35-mm glass bottom culture dishes at least 24 h before microscopy. For imaging of spread-out adherent cells, a recommended seeding density is 90,000 cells in 2 ml of DMEM supplemented with 10% FBS (*see Note 2*).
2. Confluency of HeLa cells should not exceed 50% before addition of gene vectors.

3.4. Preparation of Fluorescent Gene Carriers

Nonviral PEI/DNA gene complexes are prepared at nitrogen (NH₃⁺) to phosphate (PO₄⁻) (N/P) ratio of 10 in some preferred formulations; however, other ratios can be used. In general, excess N/P ratio beyond 6 affords rapid formation of uniformly small gene complexes in the range of 100–200 nm. The size distribution of gene vectors should be measured using, for example, dynamic light scattering.

1. Prepare working PEI solution (65 μ g/ml, 150 mM NaCl): 6.5 μ l of 1 mg/ml fluorescently labeled 25 k PEI, 7.5 μ l 1 M NaCl, 36 μ l ddH₂O.
2. Prepare working DNA solution (50 μ g/ml, 150 mM NaCl): 2.5 μ l of 1 mg/ml DNA, 7.5 μ l 1 M NaCl, 40 μ l ddH₂O.

3. Quickly add PEI drop wise to DNA, vortex for 6–8 s at medium setting. Incubate at room temperature for 15 min.
4. Remove unconjugated PEI by ultra-filtration (*see Note 3*). The solution of complexes may be filtered to remove free-PEI using any filtration device with 100,000 Da MWCO. Two additional wash and filter steps with 150 mM NaCl ensures complete removal of free-PEI. Up to 30–40% of the complexes may be lost during this process (*see Note 4*).

3.5. *MPT of Nonviral Gene Complexes in Fresh Human Mucus*

1. Collect fresh mucus samples (refer to **Subheading 2.2.** for details). Store mucus at 4 °C in dark before use (for fresh mucus) or at –20 °C (for long-term storage). For fresh mucus, do not store sample for more than 2 h before use.
2. On the basis of the total volume of the mucus sample, add up to 3% v/v of particle solution into the core of the sample. Do not attempt to facilitate mixing of particles by stirring with pipet tips, as rigorous stirring may disrupt and shear mucus fiber networks (*see Note 5*).
3. Carefully transfer 400–500 μ l of the sample to one of the chambers in a 4-well glass chamber slide and minimize formation of air bubbles (*see Note 6*). Equilibrate at room temperature in dark for 2 h.
4. Perform microscopy as outlined in **Subheading 3.2, steps 4–5**. At high gene vector concentrations, the gene vector may exert sufficient attractive forces with mucus fibers to collapse the mucus network into bundles, which can be observed directly under the microscope. In such cases, the concentration of gene vectors should be diluted.

3.6. *MPT of Nonviral Gene Complexes in Live Cells*

1. Add 20 μ l of freshly prepared DNA/polymer nanocomplexes to cell media. Gently swirl the glass bottom chamber to facilitate mixing of complexes in media. Place back in cell culture incubator for the duration of incubation desired. For nonviral gene vectors, a minimum of 15–30 min is typically required.
2. Add 2 μ l of Hoechst 34580 30 min before microscopy (*see Notes 7 and 8*).
3. Warm the observation area of the microscope with a stage warmer (preferably a live cell chamber) to 37 °C.
4. Gently wash cells (2 ml) thrice with warm (37 °C) PBS to remove non-internalized gene vectors (*see Note 9*).
5. Replace media with phenol red-free OptiMEM (2 ml).
6. Place sample under microscope for observation. Ensure that the temperature (37 °C) is maintained if using a blower. Identify the cell layer.
7. Perform a z-stack with dual channel imaging of UV and FITC scan to record location of gene carriers with respect to nucleus.
8. Obtain movies at desired spatiotemporal resolution, usually maximum.

3.7. Obtaining Displacements of Latex Beads and Gene Complexes

The process for obtaining particle trajectories from movies is similar despite various programs available to accomplish such tasks. In general, it involves identifying the first point of the trajectory for each particle, and the centroid of each particle as it moves across different frames is calculated based on algorithms that identify the outline and maximum intensity of fluorescence within a defined neighboring space (19). The protocol described below is specific to the Metamorph software 6.1.

1. Open the movie file in Metamorph. Confirm the number of frames imported matches the duration of the movie.
2. Create regions highlighting the area of interest. For particle tracking in cells, the region should encompass each cell; for particle tracking in glycerol or other extracellular fluids, four equal size regions should be used to evenly divide the tracking area.
3. Select a region, zoom-in 400%, then select Edit → Duplicate → Stack with Zoom (see Note 10).
4. Open the Track Objects Application. Use the Template Match algorithm. Select to only output object number, frame number, x and y positions.
5. Select Track, then highlight particles to be tracked. Ensure the inner box highlights only the fluorescent pixels from each particle. The outer box denotes the area where the algorithm will search for the particle in the next frame; as a general rule of thumb, the dimensions of the outer box should be roughly three times larger than the inner box. After selecting all particles to be tracked, hit OK to proceed.
6. Export the outputted information (Object number, frame number, x , y) into either an Excel or a text file.

3.8. Translating x , y Positional Data Over Time for Calculation of Mean Squared Displacements and Effective Diffusivities

The actual implementation of programming software to calculate displacements is both program and user dependent, and the steps below only outline the calculations needed. A distribution of the C++ implementation, without support, is available upon request to hanes@jhu.edu.

1. Import the particle frames and position data.
2. Calculate the geometric average of mean squared displacements for all particles across all time scales. This is a key and perhaps most confusing step in the analysis. The MSD at the shortest time scale of each particle is strictly the arithmetic mean of squared displacements for that particle across every frame, $MSD = (x_{n+1} - x_n)^2 + (y_{n+1} - y_n)^2$, where n represents the frame number. For the ensemble averaged MSD across the entire particle population, a geometric mean over all particle MSD at each time scale should be used to minimize effects of

outliers. When calculating MSD at other time scales, it is important to note that frame number and time scale are independent of each other. For example, MSD at a temporal resolution four times greater than the shortest temporal resolution does not imply calculating displacements between every fourth frame (i.e., $1 \rightarrow 5$, $5 \rightarrow 9$, $9 \rightarrow 13 \dots$). Rather, it involves calculating the displacements between all frames that are a defined temporal resolution apart. Thus, MSD at a temporal resolution four times greater than the shortest temporal resolution is an arithmetic average of displacements between frame $1 \rightarrow 5$, $2 \rightarrow 6$, $3 \rightarrow 7$, etc.

3. Calculating the effective diffusivities (D_{eff}). Once the geometric MSD across all time scales is calculated, the $D_{\text{eff}}(\tau)$ is simply $D_{\text{eff}}(\tau) = \text{MSD}(\tau)/(4\tau)$.

3.9. Measuring the Tracking Resolution

There are two common methods to calculate the resolution of the microscope; fluorescently labeled particles can either be glued to the glass chamber and the thermal motions measured (**I5**), or the particles can be suspended in a homogeneous viscous fluid such as glycerol (**I**). The latter offers the advantage of accounting for errors arising from implementation of algorithms used in locating centroids of particles from frame to frame.

1. Following the steps outlined in **Subheadings 3.2, 3.7, and 3.8**, obtain a log-log plot of MSD vs. time scale τ .
2. Using any graphing software (e.g., Microsoft Excel), fit the data to the equation $\text{MSD} = 4D_o\tau + 4\sigma^2$, where σ is the tracking resolution. The resolution for well-aligned microscopes typically varies between 5 and 10 nm.

3.10. Characterizing the Mechanism of Transport

As discussed in the introduction, gene vectors in biological environments may undergo episodes of hindered transport, unobstructed diffusion, and facilitated active transport. Despite the ambiguity, it is possible to distinguish particles that move substantially faster or slower than diffusive particles by analyzing the Relative Change in effective diffusivity (RC). This method was first presented for the analysis of transport of particles microinjected in the cytoplasm of live carcinoma cells (**9**) and for comparing the transport of viral and nonviral gene vectors in live primary neurons (**I8**). RC values are defined as $\text{RC} = D_{\text{eff}}(\tau^{\text{comp}})/D_{\text{eff}}(\tau^{\text{ref}})$, where τ^{comp} is the comparison time scale and τ^{ref} represents the reference time scale. For a population of purely Brownian particles, the RC values have a Gaussian distribution around 1. This classification scheme thus differentiates mechanisms of particle movements by considering the deviation of RC values of individual particles from Brownian behavior at short and long time scales. The analysis involves three major steps: (1) establishing the range of RC values describing diffusive transport at short and long

time scales, (2) calculating the RC values of individual particles at short and long time scales, and (3) comparing the RC values of particles to the RC range to determine the mechanism of transport. These steps are illustrated in **Fig. 2**. Comparison of the mode of particle transport at short and long time scales affords an improved understanding of the dominant mechanism across different time scales. The overall mechanism of transport over time scale is classified based on the scheme presented in **Fig. 2**. It is important to note that this classification method strictly determines the mechanism of transport. All purely diffusive motions, regardless of the bulk fluid viscosity, would be similarly classified as diffusive.

An RC curve represents the range of relative effective diffusivities across time scale where a particle exhibits random walk behavior (*see Fig. 2*). Data of purely Brownian diffusion can be created through Monte Carlo simulation of random walks or from particle tracking in glycerol (*see Note 11*). The factors affecting the RC curve are time scale and the confidence interval with which

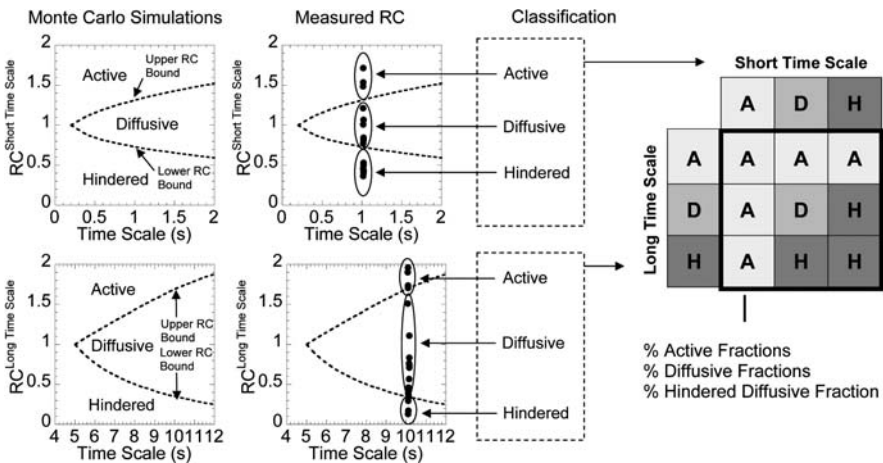


Fig. 2. Flow chart depicting the process of classifying overall transport mode of particle motions into hindered-diffusive, diffusive, and active based on the mechanism of transport at short and long time scale. On the basis of Monte Carlo simulations, an RC master curve mapping the range of RC values characterizing 95% of Brownian motions as diffusive over short and long time scale is established. Next, the experimentally obtained RC values are compared to the RC master curve. RC values above the upper RC bound are classified as active, within the RC bounds as diffusive, and below the lower RC bound as hindered-diffusive. Using this strategy, the transport modes over respective short and long time scale are obtained. Finally, the overall mechanism of gene vector transport across all time scales is determined based on the above classification scheme.

a particle is to be classified as Brownian. We have conveniently set this value at 95%, where the fastest 2.5% of particles may be mis-classified as actively transported and the slowest 2.5% as undergoing hindered diffusion. Monte Carlo simulations are preferred, as the sample size is not only much greater (e.g., 100,000 random walks are typically simulated compared to 100s of trajectories from particle tracking in glycerol) but also free of experimental error.

1. Monte Carlo simulation of random walks. The easiest method is to simulate sequential displacements of fixed length in random directions for a defined number of steps ($x_{n+1} = x_n + d \cos(\theta)$, $y_{n+1} = y_n + d \sin(\theta)$, where d is the fixed length (typically set as 1) and θ is generated from a random number generator). Then, perform the analysis discussed in **Subheading 3.8**. The unit length of motion is irrelevant as we are only calculating for the relative change in effective diffusivities. At least $n = 100,000$ trajectories should be simulated.
2. Calculate the RC values of simulated random walk using the equation $RC = D_{\text{eff}}(\tau^{\text{comp}})/D_{\text{eff}}(\tau^{\text{ref}})$, and sort the RC values in increasing order. The RC value dividing the lowest 2.5% of particles from the remaining 97.5% is considered lower RC range; the RC value dividing the highest 2.5% is considered the upper RC range. (Note: The choice of time scale considered as short or long depends on the fluid and particles used and is best decided by an expert. Typically, the short time scale transport mode is established at $RC = D_{\text{eff}}(5T)/D_{\text{eff}}(T)$, where T represents the smallest time scale. The long time scale transport mode is calculated at $RC = D_{\text{eff}}(50T)/D_{\text{eff}}(25T)$. It is important to confirm that a particular choice of time scale has little effect on the overall classification of particle transport. The temporal difference between the comparison and reference time scales should not be too large, as the ability to distinguish hindered motions is reduced at long time scales.
3. Calculate the RC values of experimental data in the same fashion as **step 2**.
4. Compare the RC values at both short and long time scales from experimental data to the RC range established in **step 2**. Particle RC value below the lower RC range is considered hindered diffusive and above the upper RC range is active transport. The predominant transport mechanism for each particle is classified from the mechanism at short and long time scales following **Fig. 2**.
5. Calculate the number of particles exhibiting an overall transport mechanism of hindered, diffusive, and active (*see Note 12*).

4. Notes

1. Movement of particles out of the plane of focus is rare for short movies in a viscoelastic environment, such as the cell cytoplasm or mucus. However, even if particles do move away from the plane of focus, the apparent size increase of particles should be of no consequence in microscopes that are well aligned as these out-of-plane movements should not translate into artificial x - y movements of the centroid of the particles.

2. To achieve simultaneous imaging with fluorescently labeled organelles through plasmids expressing fluorescently labeled proteins (e.g., EEA1-GFP fusion protein for labeling of early sorting endosomes), cells may be pre-transfected using electroporation. In such scenarios, electroporated cells should be plated >24 h before microscopy with a seeding density of 150,000 cells per 2 ml FBS-supplemented media.
3. This step ensures that the fluorescence detected during microscopy is not due to fluorescence of free polymers but of the actual gene vectors. From our experience, the intracellular transport of common gene vectors following either polymer fluorescence or DNA fluorescence is similar, so this purification process may not be necessary in some cases.
4. If maintaining the same concentration of complexes is important, the concentration of complexes in solution can be measured on a UV spectrophotometer for absorbance at 260 nm. Conjugation of DNA with cationic polymers, such as PEI, has no effect on A_{260} readings.
5. The exact volume of mucus is often difficult to determine because of its highly viscoelastic nature. However, estimation using a density of 1 g/ml is generally sufficient. The volume of particles to add is up to 3% v/v in such a scenario.
6. If using an 8-well glass chamber slide, the volume can be reduced to 200–300 μ l. It may be difficult to transfer highly viscoelastic mucus using a typical 1 ml pipet tip. In such cases, a 1-ml syringe is recommended for transfer of mucus to glass chamber slides.
7. To achieve simultaneous imaging with fluorescently labeled organelles, ex vivo dyes (e.g., LysoTracker, FM 4-64, etc.) may be added 30 min to 1 h before microscopy.
8. Microtubules are typically involved in the intracellular facilitated active transport observed for most viruses and nonviral gene vectors (*I*). To test whether the intracellular transport of specific gene vectors is dependent on microtubules, add 10 μ g/ml nocodazole in the media 1 h before microscopy to depolymerize the microtubule network.
9. An additional round of acid wash before PBS washes may be included as well. Acid washes have been shown effective at removing membrane-bound objects. To confirm viability of live cells in the presence of gene vectors, a wash step with 0.4% w/v of Trypan blue (1 ml) for 30 s followed by three more washes with PBS can be added. Trypan blue is excluded from the plasma membrane of live cells; the viability of cells can be directly observed under a light microscope. Do not add Hoechst dyes for nucleus labeling if performing Trypan blue wash step. Trypan blue has the added advantage of reducing green fluorescence and can reduce green fluorescence signals of particles adhering to surface of cells or in dead cells.
10. This step increases the number of pixels in the tracking movie by 4 \times in each dimension, with intensity of new pixels an extrapolation of surrounding pixel intensities. While no new information is introduced, this step aids in achieving

better resolution of the particle tracking analysis by reducing the discreet pixel size.

11. We have analyzed the motion of hundreds of particles in glycerol using the classification scheme from Monte Carlo simulations and found correct classification of transport modes within the confidence interval.
12. To confirm the accuracy of the transport mode classification, plots of geometric MSD vs. time scale should be plotted for each group. The slope of the data on such plot should be <1 for hindered diffusion, ~ 1 for diffusive, and >1 for active.

Acknowledgments

The authors gratefully acknowledge financial support from the National Institute of Health (NIH IROIEB00358-01) the National Science Foundation (NSF BES0346716) and a post-graduate scholarship (PGSD) from the Natural Science and Engineering Research Council of Canada (SKL). The authors thank Sudhir Khetan, Jung Soo Suk, and Kaoru Hida for critical review.

References

1. Suh, J., Dawson, M., and Hanes, J. (2005) Real-time multiple-particle tracking: applications to drug and gene delivery. *Adv Drug Deliv Rev* **57**, 63–78.
2. Riordan, J. R., Rommens, J. M., Kerem, B., Alon, N., Rozmahel, R., Grzelczak, Z., et al. (1989) Identification of the cystic fibrosis gene: cloning and characterization of complementary DNA. *Science* **245**, 1066–73.
3. Hanes, J., Dawson, M., Har-el, Y., Suh, J., and Fiegel, J. (2003) Gene Delivery to the Lung. *Pharmaceutical Inhalation Aerosol Technology*, A.J. Hickey, Editor. Marcel Dekker Inc., New York, pp. 489–539.
4. Powell, K., and Zeitlin, P. L. (2002) Therapeutic approaches to repair defects in DeltaF508 CFTR folding and cellular targeting. *Adv Drug Deliv Rev* **54**, 1395–408.
5. Dawson, M., Wirtz, D., and Hanes, J. (2003) Enhanced viscoelasticity of human cystic fibrotic sputum correlates with increasing microheterogeneity in particle transport. *J Biol Chem* **278**, 50393–401.
6. Lai, S. K., O'Hanlon, E. D., Harrold, S., Man, S. T., Wang, Y. Y., Cone, R. A., et al. Rapid transport of large polymeric nanoparticles in fresh undiluted human mucus. *Proc Natl Acad Sci USA* **104**, 1482–7.
7. Dawson, M., Krauland, E., Wirtz, D., and Hanes, J. (2004) Transport of polymeric nanoparticle gene carriers in gastric mucus. *Biotechnol Prog* **20**, 851–7.
8. Suh, J., Wirtz, D., and Hanes, J. (2003) Efficient active transport of gene nanocarriers to the cell nucleus. *Proc Natl Acad Sci USA* **100**, 3878–82.
9. Suh, J., Choy, K. L., Lai, S. K., Suk, J. S., Tang, B., Prabhu, S., et al. PEGylation of nanoparticles improves their cytoplasmic transport. *Int J Nanomed* **2**(4), 1–7.
10. Suh, J., Wirtz, D., and Hanes, J. (2004) Real-time intracellular transport of gene nanocarriers studied by multiple particle tracking. *Biotechnol Prog* **20**, 598–602.

11. Lukacs, G. L., Haggie, P., Seksek, O., Lechardeur, D., Freedman, N., and Verkman, A. S. (2000) Size-dependent DNA mobility in cytoplasm and nucleus. *J Biol Chem* **275**, 1625–9.
12. Kusumi, A., Sako, Y., and Yamamoto, M. (1993) Confined lateral diffusion of membrane receptors as studied by single particle tracking (nanovid microscopy). Effects of calcium-induced differentiation in cultured epithelial cells. *Biophys J* **65**, 2021–40.
13. Anderson, C. M., Georgiou, G. N., Morrison, I. E., Stevenson, G. V., and Cherry, R. J. (1992) Tracking of cell surface receptors by fluorescence digital imaging microscopy using a charge-coupled device camera. Low-density lipoprotein and influenza virus receptor mobility at 4 degrees C. *J Cell Sci* **101**(Pt 2), 415–25.
14. Seisenberger, G., Ried, M. U., Endress, T., Buning, H., Hallek, M., and Brauchle, C. (2001) Real-time single-molecule imaging of the infection pathway of an adeno-associated virus. *Science* **294**, 1929–32.
15. Apgar, J., Tseng, Y., Fedorov, E., Herwig, M. B., Almo, S. C., and Wirtz, D. (2000) Multiple-particle tracking measurements of heterogeneities in solutions of actin filaments and actin bundles. *Biophys J* **79**, 1095–106.
16. Saxton, M. J. (1996) Anomalous diffusion due to binding: a Monte Carlo study. *Biophys J* **70**, 1250–62.
17. Saxton, M. J. (1994) Anomalous diffusion due to obstacles: a Monte Carlo study. *Biophys J* **66**, 394–401.
18. Suk, J., Suh, J., Lai, S. K., and Hanes, J. Quantifying the Intracellular transport of viral and nonviral gene vectors in primary neurons. *Exp Biol Med* **232**(3), 461–9.
19. Savin, T., and Doyle, P. S. (2005) Static and dynamic errors in particle tracking microrheology. *Biophys J* **88**, 623–38.